ANALYSIS OF ADSORBED NATURAL GAS STORAGE: LUMPED FORMULATION AND DEVELOPMENT OF DIMENSIONLESS GROUPS

M.J.M. da Silva, mjmoraes@gmail.com
M.S.M. Pinto, marcos.smp@gmail.com
D.S. Jurumenha, diegojurumenha@hotmail.com
L.A. Sphaier, lasphaier@mec.uff.br
Laboratório de Mecânica Teórica e Aplicada, Programa de Pós-Graduação em Engenharia Mecânica, Departamento de Engenharia Mecânica, Universidade Federal Fluminense, Rua Passo da Pátria 156, bloco E, sala 216, Niterói, RJ, 24210-240, Brazil

Abstract. *Adsorbed natural gas (ANG) vessels have been shown to be an attractive alternative to compressed natural gas (CNG) or liquefied natural gas (LNG), on various circumstances. However, in spite of the advantages associated with ANG over other storage modes, there are some issues that need be properly addressed in order to ensure a viable employment of such alternative. For instance, the thermal effects resulting of adsorption and desorption, tend to diminish the storage capacity, thereby resulting in poorer performance. Hence, the heat and mass transfer mechanisms that occur in these devices must be carefully analyzed. In this study, a simple mathematical model was proposed, followed by a coherent normalization scheme, leading to previously unseen dimensionless groups. The process of charging ANG (adsorbed natural gas) cylinders was simulated employing the proposed formulation, and satisfactory results were obtained. The non-dimensional analysis introduced characteristic heat and mass transfer parameters, leading to a new perspective to GNA research.*

Keywords: *Natural Gas; Adsorption; Heat and mass transfer; Lumped Formulation*

1. NOMENCLATURE

c_p	constant pressure specific heat
CR	performance coefficient
C*	thermal capacity ratio
i	specific enthalpy
i_{sor}	heat of sorption
H*	dimensionless heat transfer coefficient
m	mass
$\dot{m}$	mass flow rate
M_l^*	adsorbed fraction
p	pressure
u	specific internal energy
t	time
T	temperature
$\mathcal{V}$	reservoir volume
(V/V)	volumetric ratio

Greek Symbols	
ρ	specific mass
ϵ	porosity
Subscripts	
e	effective or apparent
g	gas phase
i	inter-particle voids
l	adsorbed (liquid) phase
s	solid phase
p	particle
w	reservoir wall
μ	micro-pores
λ	meso-pores
κ	macro-pores
T	isothermal operation

2. INTRODUCTION

The problem of natural gas storage and transportation has been shown to have a significant importance in several areas. The current storage and transportation methods for natural gas are compressed natural gas (CNG) and liquefied natural gas (LNG). Compressed gas has the disadvantage of working at high pressures, which require heavy reservoirs for transportation and high compression costs. On the other hand, liquefied gas needs cryogenic temperatures and specialized equipment for re-gasification. Adsorbed natural gas (ANG) comes as promising technology for storage and transportation since lower pressures are employed and there is no need for extreme temperature reductions. Compared to CNG this means that equivalent storage capacities are feasible at lower pressures, thereby reducing compression costs.

The main problem with adsorbed natural gas is that the sorption heating (and cooling) effect degrades the storage capability, and hence thermal analyses have been proposed with the goal of optimizing thermal performance for reducing these unwanted heating effects. In this context a number of studies have been carried out. Wegrzyn and Gurevich (1996) compare adsorbed natural gas storage with CNG and GNL, providing estimates of costs associated to each technology. Alcañiz-Monge, de la Casa-Lillo et al. (1997) experimentally investigated the problem of methane storage in two series of activated carbon fibers. Mota, Rodrigues et al. (1997a,b) provided a mathematical model for evaluating charge and discharge dynamics of adsorbed methane. The study (Mota, Rodrigues et al., 1997a) is specifically focused on examining the effects of intra-particle diffusion. Vasiliev, Kanonchik et al. (2000) simulate the use of a heat pipe to reduce the unwanted thermal effects. The authors use a model that take into account temperature variations in radial and axial directions, but the gas concentration only in the radial direction. Methane storage is considered and the Dubinin and Radushkevich equation of the state is used.

Keller, Dreisbach et al. (1999) provides a panoramic view of classic and new methods for measuring adsorption isotherms for multi-component gases on microporous solids. Biloe, Goetz et al. (2001) performs a characterization of adsorbent composite blocks for methane storage, and Biloé, Goetz et al. (2002) employ the Dubinin-Astakhov isotherm relation for methane to determine the influence of microporous characteristics of activated carbon on both charge and discharge of a ANG system. Experimental results are also provided for validation. Zhou (1997) presents a lumped formulation for simulating the thermal effects in the slow and continuous depressurization of compressed and adsorbed gas vessels. The model only includes energy balance equations with constant coefficients, leading to analytical solutions.

In spite of the relevance of the aforementioned studies, all of them are limited with respect to normalization of the problems. As a matter of fact, apparently, no previous studies encountered in the literature present a discussion on the dimensionless groups relevant to this type of problem. In this context, the purpose of this paper is to provide a meaningful presentation of dimensionless parameters associated to the problem of heat and mass transfer in adsorbed natural gas storage. Simulation results of a lumped formulation are presented to illustrate the dependence of the dimensionless parameters on the (thermal) performance. With the normalized formulation the analysis of the problem can be much simplified, and it will thus help with the improvement of storage performance in ANG reservoirs.

3. PROBLEM FORMULATION

3.1 Volumes, porosities and concentrations

The problem of natural gas storage using adsorption, involves the transport of heat and mass within a reservoir which is filled with a porous adsorbent. The resulting porous material that fills the reservoir may composed of adsorbent particles or appear in a monolithic form. In either way, the reservoir will end up having an effective or total porosity. The reservoir volume $\mathcal{V}$ can be subdivided, in a general form, in:

$$\mathcal{V} = \mathcal{V}_s + \mathcal{V}_\delta + \mathcal{V}_i + \mathcal{V}_\pi = \mathcal{V}_p + \mathcal{V}_i \tag{1}$$

where $\mathcal{V}_i + \mathcal{V}_\pi$ is the total usable void volume (the fraction of $\mathcal{V}$ that could be filled with natural gas). The dead-end pores have no effect on mass transfer and hence the effectively useful (interconnected) void volume excludes $\mathcal{V}_\delta$. The volume $\mathcal{V}_p$ is the particle volume and the inter-particle void space $\mathcal{V}_i$ is null for a monolithic material. Assuming that void spaces are uniformly distributed within the porous medium, the total (usable) porosity, the bed porosity (assuming that the medium is composed of porous particles) and the particle (or monolithic) porosity are defined as:

$$\epsilon = \frac{\mathcal{V}_i + \mathcal{V}_\pi}{\mathcal{V}}, \qquad \epsilon_b = \frac{\mathcal{V}_i}{\mathcal{V}}, \qquad \epsilon_p = \frac{\mathcal{V}_\pi}{\mathcal{V}_p}, \tag{2}$$

where $\epsilon_b = 0$ for a monolithic material. The total porosity is related to the bed and particle porosities as:

$$(1 - \epsilon) = (1 - \epsilon_b)\,(1 - \epsilon_p). \tag{3}$$

The skeletal volume of the particle (or a monolithic material) is defined as the volume fraction occupied by the voidless solid and closed-pores; hence the skeletal fraction can be written as:

$$\frac{\mathcal{V}_s + \mathcal{V}_\delta}{\mathcal{V}_p} = 1 - \epsilon_p. \tag{4}$$

Assuming that the mass of solid is uniformly distributed within the medium, the skeletal density (also called true density), which includes the volume of voidless solid and closed-pores, is defined as:

$$\rho_s = \frac{m_s}{\mathcal{V}_s + \mathcal{V}_\delta}. \tag{5}$$

The bulk volume of the porous solid material is defined in terms of the total volume:

$$\rho_b = \frac{m_s}{\mathcal{V}} = \rho_s\,(1 - \epsilon_b)\,(1 - \epsilon_p) = \rho_s\,(1 - \epsilon). \tag{6}$$

The concentration of the gaseous phase is written in terms of void spaces excluding closed-pores:

$$\rho_g = \frac{\delta m_g}{\delta \mathcal{V}_g}, \tag{7}$$

whereas the adsorbed phase concentration is defined in terms of the total volume:

$$\rho_l = \frac{\delta m_l}{\delta \mathcal{V}}. \tag{8}$$

Hence, infinitesimal masses of gas and liquid (adsorbate) can be written as:

$$\delta m_g = \rho_g \, \delta \mathcal{V}_g = \epsilon \, \rho_g \, \delta \mathcal{V}, \tag{9}$$

$$\delta m_l = \rho_l \, \delta \mathcal{V}. \tag{10}$$

The concentrations ρ_g and ρ_l can be expressed in terms of temperature and pressure by introducing a equation of state and an adsorption isotherm (or equilibrium relation). The specific mass of the gaseous phase is written as:

$$\rho_g = \rho_g(T, p) = \frac{p}{R\,T}, \tag{11}$$

where the second equality stands for ideal gas behavior. The specific mass of the adsorbed phase is written in terms of an isotherm relation:

$$\rho_l = \rho_l(T, p), \tag{12}$$

in which the functional form can depend on the selected adsorbent. Following (Mota, Rodrigues et al., 1997a,b), a Langmuir adsorption isotherm is adopted:

$$\frac{\rho_l}{\rho_b} = q_m \, \frac{b\,p}{1 + b\,p}, \qquad \text{with} \qquad q_m = 55920\, T^{-2.3}, \qquad b = 1.0863 \times 10^{-7} \exp(806/T). \tag{13}$$

3.2 Mass and energy balances

A lumped mass conservation balance for the natural gas can be written as:

$$\frac{\mathrm{d}m_g}{\mathrm{d}t} + \frac{\mathrm{d}m_l}{\mathrm{d}t} = \dot{m}_g, \tag{14}$$

where $\dot{m}_g$ represents the net mass flow rate into the reservoir. The following equation is obtained for the mass balance in the reservoir.

$$\epsilon \, \frac{\mathrm{d}\bar{\rho}_g}{\mathrm{d}t} + \frac{\mathrm{d}\bar{\rho}_l}{\mathrm{d}t} = \frac{\dot{m}_g}{\mathcal{V}}. \tag{15}$$

A lumped energy balance for the natural gas reservoir can be written as:

$$\left(\epsilon \, \frac{\mathrm{d}}{\mathrm{d}t}(\bar{u}_g \, \bar{\rho}_g) + \frac{\mathrm{d}}{\mathrm{d}t}(\bar{u}_l \, \bar{\rho}_l) + \frac{\mathrm{d}}{\mathrm{d}t}(\bar{u}_s \, \rho_b) \right) \mathcal{V} + m_w \frac{\mathrm{d}\bar{u}_w}{\mathrm{d}t} = \dot{Q} + (i_g \, \dot{m}_g)|_{in}, \tag{16}$$

which can be written in terms of enthalpies

$$\left(\epsilon \, \frac{\mathrm{d}}{\mathrm{d}t}(\bar{\imath}_g \, \bar{\rho}_g) - \epsilon \, \frac{\mathrm{d}\bar{p}}{\mathrm{d}t} + \frac{\mathrm{d}}{\mathrm{d}t}(\bar{\imath}_l \, \bar{\rho}_l) + \frac{\mathrm{d}}{\mathrm{d}t}(\bar{\imath}_s \, \rho_b) \right) \mathcal{V} + m_w \frac{\mathrm{d}\bar{u}_w}{\mathrm{d}t} = \dot{Q} + (i_g \, \dot{m}_g)|_{in}. \tag{17}$$

Combining the above equation with the mass conservation formula (15), one finds:

$$\left(\epsilon \, \bar{\rho}_g \, \frac{\mathrm{d}\,\bar{\imath}_g}{\mathrm{d}t} - \epsilon \, \frac{\mathrm{d}\bar{p}}{\mathrm{d}t} + \bar{\rho}_l \, \frac{\mathrm{d}\bar{\imath}_l}{\mathrm{d}t} + (\bar{\imath}_l - \bar{\imath}_g) \, \frac{\mathrm{d}\bar{\rho}_l}{\mathrm{d}t} + \rho_b \, \frac{\mathrm{d}\bar{\imath}_s}{\mathrm{d}t} \right) \mathcal{V} + m_w \frac{\mathrm{d}\bar{u}_w}{\mathrm{d}t} = \dot{Q} + (i_g|_{in} - \bar{\imath}_g) \, \dot{m}_g. \tag{18}$$

Introducing the definition of the differential heat of sorption (Close and Banks, 1972)

$$\bar{\imath}_{sor} = \bar{\imath}_g - \bar{\imath}_l, \tag{19}$$

and relations involving specific heats

$$\mathrm{d}\bar{\imath}_g = c_{p_g} \, \mathrm{d}\bar{T} + (1 - \beta\,\bar{T}) \, \frac{1}{\bar{\rho}_g} \, \mathrm{d}\bar{p}, \qquad \mathrm{d}\bar{\imath}_l = c_l \, \mathrm{d}\bar{T}, \qquad \mathrm{d}\bar{\imath}_s = c_s \, \mathrm{d}\bar{T}, \qquad \mathrm{d}\bar{u}_w = c_w \, \mathrm{d}\bar{T}, \tag{20}$$

one arrives at:

$$\rho_e \, c_e \, \frac{\mathrm{d}\bar{T}}{\mathrm{d}t} = \frac{\dot{Q}}{\mathcal{V}} + \epsilon \, \beta \, \bar{T} \, \frac{\mathrm{d}\bar{p}}{\mathrm{d}t} + \bar{\imath}_{sor} \, \frac{\mathrm{d}\bar{\rho}_l}{\mathrm{d}t} + \Delta\bar{\imath}_g \, \dot{m}_g, \tag{21}$$

where $\rho_e\, c_e$ is the effective (or apparent) thermal capacity:

$$\rho_e\, c_e \,=\, (\rho_b\, c_s + \rho_l\, c_l) \,+\, \rho_g\, c_{p_g}\, \epsilon \,+\, \frac{m_w\, c_w}{\mathcal{V}}. \tag{22}$$

The total heat transfer at the cylinder outer surface (exchanged with the surroundings) is given by:

$$\dot{Q} \,=\, -\int_{\mathcal{A}_s} h\,(T - T_0)\, \mathrm{d}\mathcal{A} \,\approx\, -h\,(\bar{T} - T_0)\,\mathcal{A}_e, \tag{23}$$

where h is an overall heat transfer coefficient that accounts for thermal resistances within the reservoir (conductive) and at the outer surface (convective). Then, the energy equation is finally written as:

$$\rho_e\, c_e\, \frac{\mathrm{d}\bar{T}}{\mathrm{d}t} \,=\, -\,h\,(\bar{T} - T_0)\,\frac{\mathcal{A}_e}{\mathcal{V}} \,+\, \epsilon\,\beta\,\bar{T}\,\frac{\mathrm{d}\bar{p}}{\mathrm{d}t} \,+\, \bar{\imath}_{sor}\,\frac{\mathrm{d}\bar{\rho}_l}{\mathrm{d}t} \,+\, \Delta\bar{\imath}_g\,\dot{m}_g. \tag{24}$$

The term $\Delta\bar{\imath}_g$ will depend on an approximate relation between the averaged enthalpy in the reservoir and at its inlet, being given by:

$$\Delta\bar{\imath}_g \,=\, \bar{\imath}_g|_{in} - \bar{\imath}_g, \tag{25}$$

Assuming that these are approximately equal $\Delta\bar{\imath}_g \approx 0$.

The initial conditions for the following problem are given in terms of pressure and temperature:

$$\bar{p}(t=0) \,=\, p_0, \qquad \bar{T}(t=0) \,=\, T_0, \tag{26}$$

in which $p_0 = p_{\max}$ for discharge and $p_0 = p_{\min}$ for charge.

4. PERFORMANCE ASSESSMENT

In order to assess the performance of a process (either charge or discharge), the parameter CR, introduced by Mota, Rodrigues et al. (1997b), is adopted:

$$\mathrm{CR} \,\equiv\, \frac{\Delta m_{\text{real}}}{\Delta m_{\max}}, \tag{27}$$

representing a ratio between the actual amount of gas delivered during discharge (or stored, during charge), Δm_{real}, and the maximum amount that can be delivered (or stored), which occurs for isothermal operation.

The actual (real) and the ideal (isothermal) masses of NG stored can be written as:

$$\Delta m_{\text{real}} \,=\, \int_0^{t_f} |\dot{m}_g|\,\mathrm{d}t, \qquad \Delta m_{\max} \,=\, \int_0^{t_f} |\dot{m}_g|_T\,\mathrm{d}t, \tag{28}$$

in which t_f is the process (charge or discharge) time. Based on the minimum and maximum pressures one defines the maximum storage capacity:

$$\Delta m_{\max} \,=\, (\epsilon\,\Delta\rho_g \,+\, \Delta\rho_l)\,\mathcal{V}. \tag{29}$$

Naturally, for isothermal operation t_f will be the time taken for the reservoir pressure reach the critical pressure ($p_{\max}$ for charge and $p_{\min}$ for discharge).

A particular situation occurs if inlet flow rates are independent of operating conditions (*i.e.* pressure and temperature), in which the previous quantities can be written in terms of the isothermal process time and a critical time, t_c:

$$\Delta m_{\text{real}} \,=\, \int_0^{t_c} |\dot{m}_g|\,\mathrm{d}t \,+\, \int_{t_c}^{t_f} |\dot{m}_{g,cr}|\,\mathrm{d}t, \qquad \Delta m_{\max} \,=\, \int_0^{t_f} |\dot{m}_g|\,\mathrm{d}t, \tag{30}$$

in which the parameter t_c represents the instant at which the critical reservoir pressure is reached. In summary:

$$p(t_c) \,=\, p_{\max}, \qquad \text{for charge,} \tag{31}$$

$$p(t_c) \,=\, p_{\min}, \qquad \text{for discharge,} \tag{32}$$

and $\dot{m}_{g,cr}$ is the modified mass flow rate (dependent on operating conditions) due to the fact that the critical pressure has been reached. This flow rate is clearly smaller than the original one, and is what gives CR values smaller than unity.

Naturally, if a value of t_c greater than (or equal to) t_f is found, this means that the critical pressure was not reached and hence $\Delta m_{\text{real}} = \Delta m_{\text{isoth}}$, *i.e.* $\text{CR} = 1$. Also, for isothermal operation $t_c = t_f$.

A traditional parameter used to measure natural gas storage capacity is the volume ratio (V/V), defined as:

$$(V/V) \equiv \frac{\text{volume of NG (gaseous) under normal conditions}}{\text{reservoir internal volume}} = \frac{\mathcal{V}_0}{\mathcal{V}}. \tag{33}$$

It can be shown that this parameter can be alternatively calculated from:

$$(V/V) = \frac{m_{\text{real}}}{m_0}, \qquad \text{with} \qquad m_{\text{real}} = m_{\min} + \Delta m_{\text{real}} = m_{\min} + \text{CR}\,\Delta m_{\max}, \tag{34}$$

where the minimum amount of NG contained in the reservoir (for isothermal operation) and the mass of gaseous NG that fits in the reservoir under normal conditions are given by:

$$m_{\min} = (\varepsilon\,\rho_{g,\min} + \rho_{l,\min})\,\mathcal{V}, \qquad m_0 = \rho_0\,\mathcal{V}. \tag{35}$$

5. DIMENSIONLESS GROUPS

Assuming that both charge and discharge are processes that start from an initial temperature that is equilibrium with the surroundings, the initial temperature for both cases is the surroundings temperature itself, T_0. The minimum reservoir pressure (for the gas phase) occurs at the beginning of the charge cycle (or at the end of the discharge cycle). The maximum pressure occurs at the end of the charge cycle (or at the beginning of the discharge cycle). Using equation (11) minimum and maximum values of gas concentration can be written:

$$\rho_{g,\max} = \frac{p_{\max}}{R T_0}, \qquad \rho_{g,\min} = \frac{p_{\min}}{R T_0}, \tag{36}$$

where $\rho_{g,\max}$ corresponds to the gas concentration at the end of the charge cycle, or at the beginning of the discharge cycle for isothermal operation. For non-isothermal operation, this maximum value will not be reached, and hence less gas will be stored in the reservoir. In a similar fashion, $\rho_{g,\min}$ represents the gas concentration at the beginning of the charge cycle, or at the end of the discharge cycle for isothermal operation. Again, for non-isothermal operation the value of $\rho_{g,\min}$ cannot be attained during discharge, resulting a limited gas recovery.

Analogous to gas phase concentrations, minimum and maximum values of adsorbed phase concentrations are defined in terms of $p_{\min}$, $p_{\max}$ and T_0:

$$\rho_{l,\max} = \rho_{l,\max}(p_{\max}, T_0), \qquad \rho_{l,\min} = \rho_{l,\min}(p_{\min}, T_0). \tag{37}$$

Once more, some of these values can only be achieved under a isothermal operation, since the effects of heating (during charge) and cooling (during discharge) worsens gas storage and recovery. Based on the minimum and maximum values for ρ_g and ρ_l, one defines the following differences:

$$\Delta\rho_g \equiv \rho_{g,\max} - \rho_{g,\min}, \qquad \Delta\rho_l \equiv \rho_{l,\max} - \rho_{l,\min}, \tag{38}$$

representing the maximum changes in these concentrations.

The first dimensionless groups represent the fractions of gas that are stored in the gaseous form and in the adsorbed form, begin defined as:

$$\text{M}_g^* = \frac{\Delta\rho_g\,\epsilon\,\mathcal{V}}{\Delta m_{\max}}, \qquad \text{M}_l^* = \frac{\Delta\rho_l\,\mathcal{V}}{\Delta m_{\max}}. \tag{39}$$

Naturally, these parameters must always satifsfy $\text{M}_g^* + \text{M}_l^* = 1$.

The next parameters comprise thermal capacity ratios between different capacities and the thermal capacity of the amount of gas charged or discharged under isothermal conditions. In this context, the thermal capacity ratios of the adsorbent material, the reservoir wall and the minimum gas contained in the reservoir are respectively defined as:

$$\text{C}_s^* = \frac{c_s\,\rho_b\,\mathcal{V}}{c_{p_g}\,\Delta m_{\max}}, \qquad \text{C}_w^* = \frac{c_w\,m_w}{c_{p_g}\,\Delta m_{\max}}, \qquad \text{C}_{\min}^* = \frac{\left(\epsilon\,c_{p_g}\,\rho_{g,\min} + c_l\,\rho_{l,\min}\right)\mathcal{V}}{c_{p_g}\,\Delta m_{\max}}. \tag{40}$$

The ratio between the specific heats of NG in the gaseous and adsorbed phases is approximately unity:

$$c_p^* = \frac{c_l}{c_{p_g}} \approx 1. \tag{41}$$

A last, and probably one of the most relevant parameters, is the dimensionless heat transfer coefficient. It is defined in a form that resembles a number of transfer units in heat exchanger; however, the fluid heat capacity rate is the average heat capacity in or outflow rate for an isothermal process:

$$\mathrm{H}^* = \frac{h\,\mathcal{A}_e\,t_f}{c_{p_g}\,\Delta m_{\max}}. \tag{42}$$

At this point it is worth noting that although dimensionless groups for a lumped formulation are being defined, the same parameters will appear in multidimensional models, with the addition of extra parameters to account for gradients within the material.

5.1 Dimensionless governing equations

The dependent and independent variables are normalized by introducing the following dimensionless forms:

$$t^* = \frac{t}{t_f}, \qquad T^* = \frac{T}{T_0}, \qquad p^* = \frac{p - p_{\min}}{p_{\max} - p_{\min}} = \frac{p - p_{\min}}{\Delta p}, \tag{43}$$

$$\rho_g^* = \frac{\rho_g - \rho_{g,\min}}{\rho_{g,\max} - \rho_{g,\min}} = \frac{\rho_g - \rho_{g,\min}}{\Delta\rho_g}, \qquad \rho_l^* = \frac{\rho_l - \rho_{l,\min}}{\rho_{l,\max} - \rho_{l,\min}} = \frac{\rho_l - \rho_{l,\min}}{\Delta\rho_l}. \tag{44}$$

Once the previous definitions are introduced in equations (15,24), a dimensionless version of the problem is obtained:

$$\mathrm{M}_g^*\,\frac{\mathrm{d}\rho_g^*}{\mathrm{d}t^*} + \mathrm{M}_l^*\,\frac{\mathrm{d}\rho_l^*}{\mathrm{d}t^*} = \dot{m}_g^*, \tag{45}$$

$$\left(\mathrm{M}_g^*\,\rho_g^* + c_p^*\,\mathrm{M}_l^*\,\rho_l^* + \mathrm{C}^*\right)\frac{\mathrm{d}T^*}{\mathrm{d}t^*} = \mathrm{H}^*\,(1 - T^*) + \mathrm{M}_g^*\,\beta^*\,T^*\,\frac{\mathrm{d}p^*}{\mathrm{d}t^*} + \mathrm{M}_l^*\,i_{sor}^*\,\frac{\mathrm{d}\rho_l^*}{\mathrm{d}t^*}. \tag{46}$$

where C^* is the added contributions of the thermal capacity ratios:

$$\mathrm{C}^* = \mathrm{C}_{\min}^* + \mathrm{C}_s^* + \mathrm{C}_w^*. \tag{47}$$

The terms on the right hand side of the energy equation represent a competition between different effects: heat transfer to the surroundings, heating/cooling to to compression and heating/cooling due to sorption. The combination of these parameters will result in a temperature variation, which can be diminished or augmented according to the valued of the thermal capacity ratio C^*.

The remaining parameters are the dimensionless heat of sorption:

$$i_{sor}^* \equiv \frac{\bar{\imath}_{sor}}{T_0\,c_{p_g}}, \tag{48}$$

the dimensionless mass inflow (negative for outflow):

$$\dot{m}_g^* \equiv \frac{\dot{m}_g\,t_f}{\Delta m_{\max}}, \tag{49}$$

and the dimensionless thermal expansion coefficient:

$$\beta^* \equiv \frac{\beta\,\Delta p}{c_{p_g}\,\Delta\rho_g} = \frac{\kappa - 1}{\kappa}\,\frac{1}{T^*}, \tag{50}$$

where the second equality reflects the fact that ideal gas behavior is assumed ($\kappa = c_{p_g}/c_{v_g}$).

A dimensionless version of the total mass in the reservoir is defined for analyzing results:

$$m^* = \mathrm{M}_g^*\,\rho_g^* + \mathrm{M}_l^*\,\rho_l^*. \tag{51}$$

Using the normalized variables, the performance coefficient CR is written as

$$\mathrm{CR} = \frac{\Delta m_{\text{real}}^*}{\Delta m_{\max}^*}, \qquad \text{with} \qquad \Delta m_{\text{real}}^* = \int_0^1 |\dot{m}_g^*|\,\mathrm{d}t^*, \qquad \Delta m_{\max}^* = \int_0^1 |\dot{m}_g^*|_T\,\mathrm{d}t^*, \tag{52}$$

Using the mass conservation equation (45) it can be easily shown that:

$$\mathrm{CR} = \frac{(\mathrm{M}_g^*\,\rho_g^*(p^*,T^*) + \mathrm{M}_l^*\,\rho_l^*(p^*,T^*))|_{t^*=1} - (\mathrm{M}_g^*\,\rho_g^*(p^*,T^*) + \mathrm{M}_l^*\,\rho_l^*(p^*,T^*))|_{t^*=0}}{(\mathrm{M}_g^*\,\rho_g^*(p_T^*,1) + \mathrm{M}_l^*\,\rho_l^*(p_T^*,1))|_{t^*=1} - (\mathrm{M}_g^*\,\rho_g^*(p_T^*,1) + \mathrm{M}_l^*\,\rho_l^*(p_T^*,1))|_{t^*=0}}, \tag{53}$$

The volume storage ratio (V/V) can be written in terms of dimensionless parameters as:

$$(V/V) = \frac{m^*_{\min} + \mathrm{CR}}{m^*_0}, \tag{54}$$

in which the quantites $m^*_{\min}$ and m^*_0 are given by

$$m^*_{\min} \equiv \frac{m_{\min}}{\Delta m_{\max}}, \qquad m^*_0 \equiv \frac{m_0}{\Delta m_{\max}}. \tag{55}$$

6. RESULTS AND DISCUSSION

Simulation results for the current model are calculated for two different processes: discharge with a constant mass outflow rate, and charge with a constant inlet pressure. There situations reflect real situations for consumption and fueling, respectively. Both cases must take into account the fact that once the critical pressure has been reached, the mass flow rate must be interrupted. In order to achieve this condition $\dot{m}^*_g$ is given by:

$$\dot{m}^*_g = s(p^*)\,\phi(p^*), \tag{56}$$

in which $s(t^*)$ is a shut-off function which becomes zero if p^* reaches a critical value. In other words:

$$s(p^*) = 1, \qquad \text{for} \qquad 0 < p^* < 1, \tag{57}$$

$$s(p^*) = 0, \qquad \text{otherwise}, \tag{58}$$

and the function $\phi(p^*)$ will have different forms depending on the type of process:

$$s(p^*) = \alpha^*\,(p^*_{in} - p^*), \qquad \text{for charge}, \tag{59}$$

$$s(p^*) = -1, \qquad \text{for discharge}. \tag{60}$$

For the charge process, the value of p^*_{in} was selected as 1.1, and the value of α^* was calculated so that at $t = t_f$ the isothermal solution reaches full capacity, *i.e.* $p^* = 1$. Figures 1 display the results for different values of H* considering M^*_l = 0.9, i^*_{sor} = 1.5, C^* = 10, which are typical values for this type of problem. As can be seen, for smaller values of H* the temperature rise is much more pronounced and consequently the maximum pressure is reached at a much earlier stage than that of the isothermal solution. As a result, for these cases, a smaller amount of gas is charged, which will lead to a worse CR. The results for H$^* = 100$ are almost isothermal, which will lead to higher CR values.

The next set of figures (2) gives the discharge results, considering a constant mass outflow rate, for the same values of the dimensionless parameters used for simulating the charge process. As one can observe, there is a significant cooling effect for smaller values of H*, which reduces the discharge capacity, as clearly seen in the concentration results. Naturally, these cases will result in a poorer performance.

One point that is worth mentioning is that two distinct regimes can be seen in these results. The first is governed by pressure; until the critical pressure is reached p^* and m^* equal the isothermal solution. The second regime is governed by temperature, commencing after the critical pressure is reached; at this stage mass is admitted into the reservoir (at a lower rate) as heat is loss to the surroundings. If the reservoir was adiabatic, there would be no mass inflow in this second stage. A similar observation could be done for the charge solution; however the distinction between the two stages is not equally clear.

The effect of varying the dimensionless parameters on the performance coefficient CR is presented in table 1. As can be seen, the higher values of H* and C* yield the better performance. In addition, for high H* values, the effect of C* on performance becomes negligible, and vice-versa. The presented results also show the impact of varying the heat of sorption, demonstrating how increasing the heat of sorption worsens charge and discharge performance.

7. CONCLUSIONS

This paper presented a lumped formulation for adsorbed natural gas storage. In spite of the simplicity of the formulation, a consistent normalization scheme is conducted. Four relevant dimensionless groups are developed associated with different heat and mass transfer mechanisms: H*, representing the heat transfer rate to the surroundings taking into account the process time; C*, representing the relative thermal capacity; i^*_{sor}, representing the sorption heating; and finally M$^*_l$, representing the fraction of gas that is stored by adsorption (the remaining fraction would be stored by compression).

After presenting the model and dimensionless groups, simulation results for charge and discharge operation were carried out for a number of cases. The results demonstrate how higher values of C* and H* lead to greater values of the coefficient of performance CR, and show how the heat of sorption can have a degrading effect on charge and discharge processes.

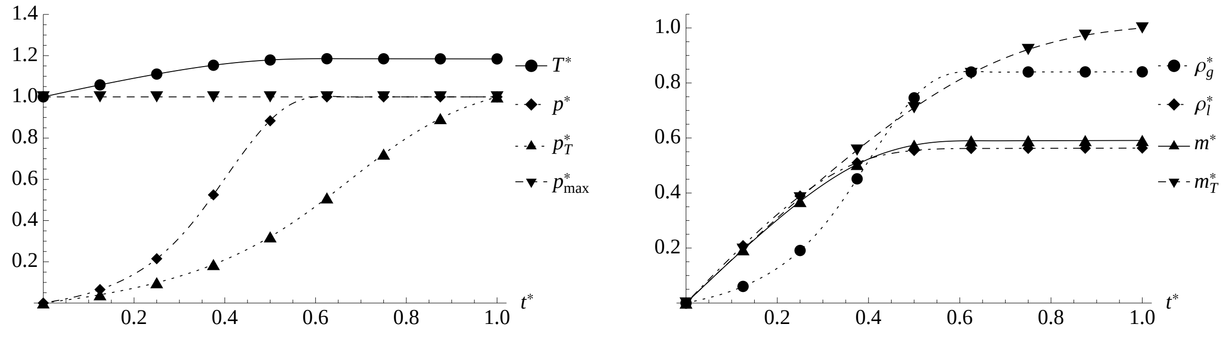

(a) T^* and p^* for charge with $\mathrm{H}^* = 0.1$.

(b) Concentrations for charge with $\mathrm{H}^* = 0.1$.

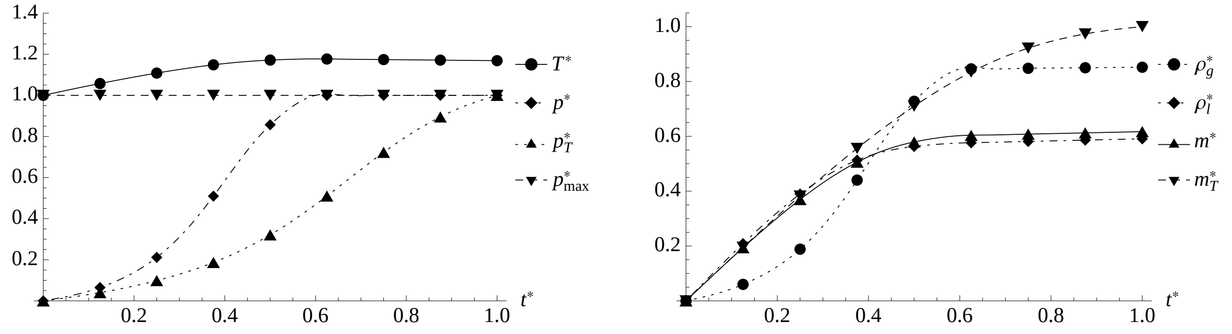

(c) T^* and p^* for charge with $\mathrm{H}^* = 1$.

(d) Concentrations for charge with $\mathrm{H}^* = 1$.

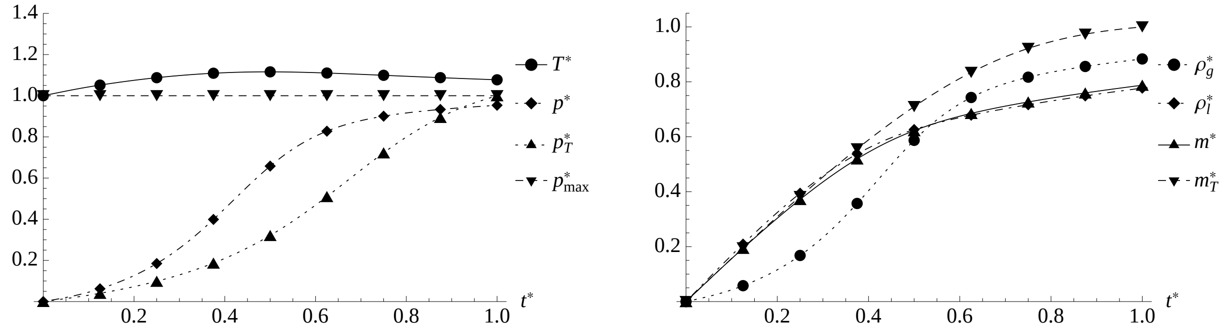

(e) T^* and p^* for charge with $\mathrm{H}^* = 10$.

(f) Concentrations for charge with $\mathrm{H}^* = 10$.

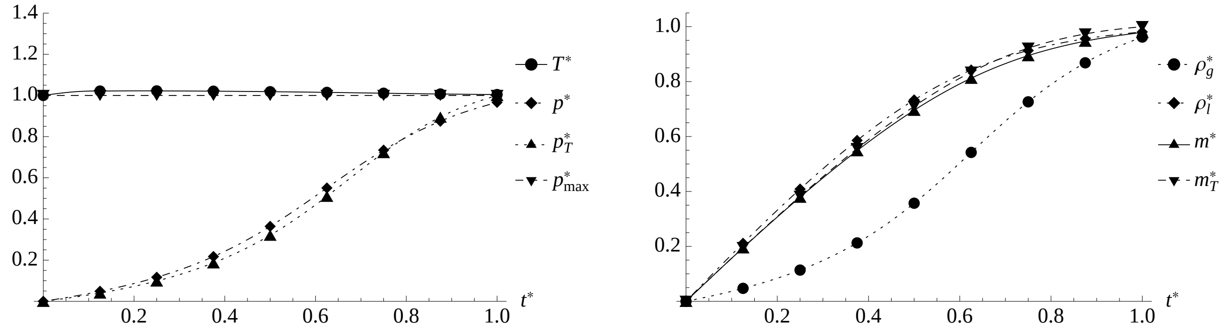

(g) T^* and p^* for charge with $\mathrm{H}^* = 100$.

(h) Concentrations for charge with $\mathrm{H}^* = 100$.

Figure 1. Pressure, temperature and concentration histories for different values of H^*: charge process.

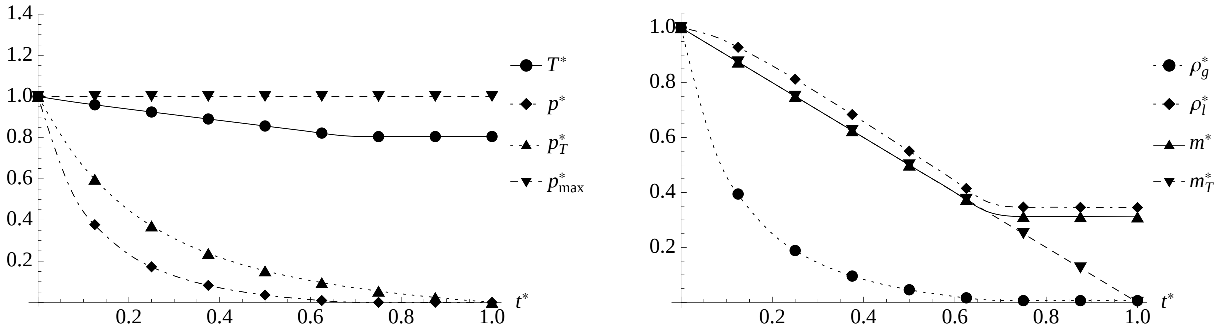

(a) T^* and p^* for discharge with $\mathrm{H}^* = 0.1$.

(b) Concentrations for discharge with $\mathrm{H}^* = 0.1$.

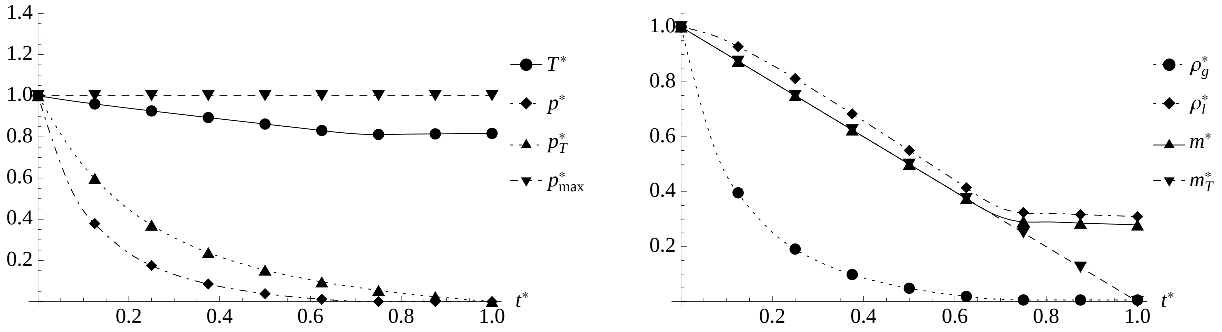

(c) T^* and p^* for discharge with $\mathrm{H}^* = 1$.

(d) Concentrations for discharge with $\mathrm{H}^* = 1$.

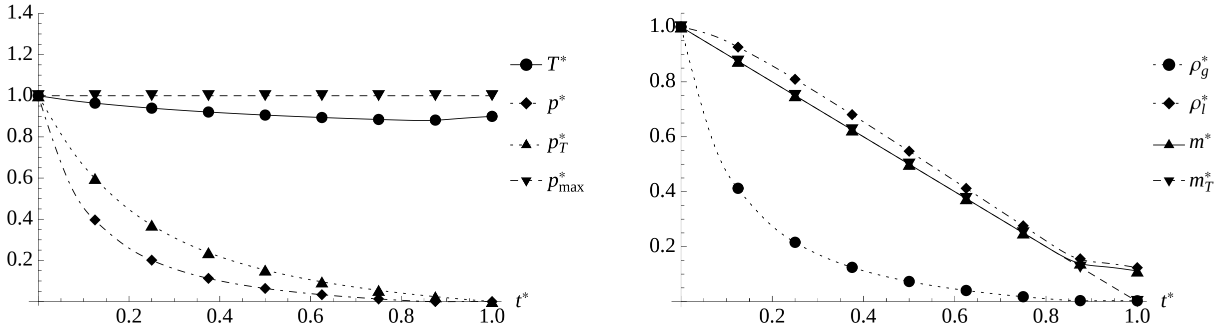

(e) T^* and p^* for discharge with $\mathrm{H}^* = 10$.

(f) Concentrations for discharge with $\mathrm{H}^* = 10$.

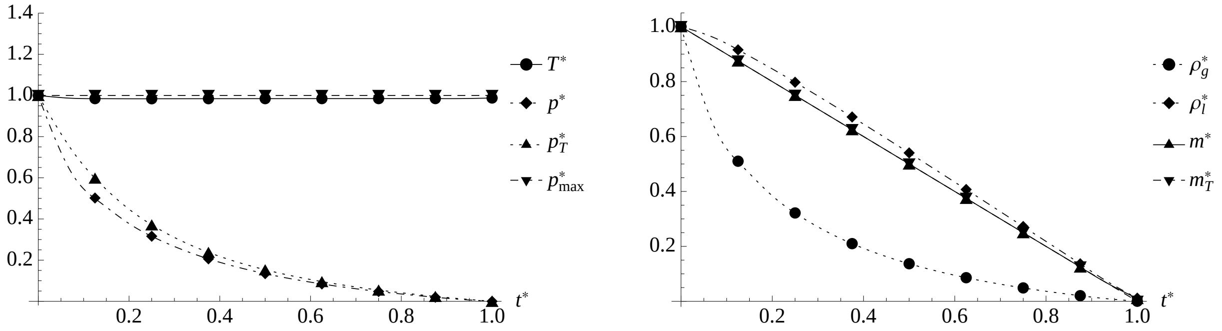

(g) T^* and p^* for discharge with $\mathrm{H}^* = 100$.

(h) Concentrations for discharge with $\mathrm{H}^* = 100$.

Figure 2. Pressure, temperature and concentration histories for different values of H^*: discharge process.

Table 1. Peformance coefficient for different configurations.

	C* for charge					C* for discharge				
H*	1	5	10	50	100	1	5	10	50	100
$i^*_{sor} = 0.5$										
0.1	0.4253	0.7454	0.8455	0.9621	0.9805	–	0.8757	0.9407	0.9889	0.9945
1	0.5436	0.7644	0.8521	0.9625	0.9806	–	0.8901	0.9440	0.9890	0.9945
10	0.8883	0.8815	0.9029	0.9660	0.9815	–	0.9578	0.9666	0.9901	0.9948
100	0.9590	0.9884	0.9870	0.9858	0.9885	–	0.9960	0.9958	0.9958	0.9968
1000	0.9672	0.9990	0.9990	0.9988	0.9987	–	0.9996	0.9996	0.9996	0.9996
10000	0.9999	0.9999	0.9999	0.9999	0.9999	–	1.0000	1.0000	1.0000	1.0000
$i^*_{sor} = 1.0$										
0.1	0.3353	0.6551	0.7762	0.9395	0.9683	0.3891	0.7786	0.8944	0.9812	0.9908
1	0.4512	0.6789	0.7854	0.9401	0.9684	0.5284	0.8034	0.9004	0.9814	0.9908
10	0.8405	0.8303	0.8576	0.9459	0.9700	0.9379	0.9234	0.9403	0.9831	0.9913
100	0.9856	0.9838	0.9814	0.9779	0.9819	0.9947	0.9927	0.9922	0.9925	0.9944
1000	0.9986	0.9986	0.9986	0.9984	0.9981	0.9995	0.9993	0.9992	0.9992	0.9992
10000	0.9999	0.9999	0.9999	0.9999	0.9999	0.9999	0.9999	0.9999	0.9999	0.9999
$i^*_{sor} = 1.5$										
0.1	0.2844	0.5910	0.7217	0.9185	0.9565	0.3138	0.6887	0.8451	0.9732	0.9870
1	0.3934	0.6171	0.7327	0.9193	0.9567	0.4286	0.7209	0.8539	0.9735	0.9870
10	0.7973	0.7878	0.8193	0.9271	0.9590	0.9082	0.8886	0.9129	0.9759	0.9876
100	0.9814	0.9789	0.9758	0.9700	0.9754	0.9928	0.9897	0.9887	0.9892	0.9920
1000	0.9983	0.9983	0.9982	0.9979	0.9976	0.9993	0.9990	0.9989	0.9988	0.9988
10000	0.9998	0.9998	0.9998	0.9998	0.9998	0.9999	0.9999	0.9999	0.9999	0.9999

8. ACKNOWLEDGEMENTS

The authors would like to acknowledge the financial support provided by, CNPq, FAPERJ, and Universidade Federal Fluminense.

9. REFERENCES

Alcañiz-Monge, J., de la Casa-Lillo, M.A., Cazorla-Amoros, D., and LinaresSolano, A., 1997, "Methane storage in activated carbon fibres", Carbon, vol. 35, no. 2, pp. 291–297.

Biloé, S., Goetz, V., and Gulliot, A., 2002, "Optimal design for activated carbon for and adsorbed natural gas storage system", Carbon, vol. 40, pp. 1295–1308.

Biloe, S., Goetz, V., and Mauran, S., 2001, "Characterization of adsorbent composite blocks for methane storage", Carbon, vol. 39, no. 11, pp. 1653–1662.

Close, D.J. and Banks, P.J., 1972, "Coupled equilibrium heat and single adsorbate transfer in fluid flow through a porous medium – II: Predictions for a silica-gel-air-drier using characteristics charts", Chemical Engineering Science, vol. 27, pp. 1157–1169.

Keller, J.U., Dreisbach, F., Rave, H., Staudt, R., and Tomalla, M., 1999, "Measurement of gas mixture adsorption equilibria of natural gas compounds on microporous sorbents", Adsorption, vol. 5, no. 3, pp. 199–214.

Mota, J.P.B., Rodrigues, A.E., Saatdjian, E., and Tondeur, D., 1997a, "Charge dynamics of methane adsorption storage system: intraparticle diffusional effects", Adsorption, vol. 3, pp. 117–125.

Mota, J.P.B., Rodrigues, A.E., Saatdjian, E., and Tondeur, D., 1997b, "Dynamics of natural gas adsorption storage system employing activated carbon", Carbon, vol. 35, no. 9, pp. 1259–1270.

Vasiliev, L.L., Kanonchik, L., Mishkinis, D., and Rabetsky, M., 2000, "Adsorbed natural gas storage and transportation vessels", International Journal of Thermal Sciences, vol. 39, pp. 1047–1055.

Wegrzyn, J. and Gurevich, M., 1996, "Adsorbent storage of natural gas", Applied Energy, vol. 55, no. 2, pp. 71–83.

Zhou, Z.W., 1997, "Thermal analysis of slow discharge from a pressurized natural gas storage tank", Applied Thermal Engineering, vol. 17, no. 11, pp. 1099–1110.

10. RESPONSIBILITY NOTICE

The authors are the only responsible for the printed material included in this paper.